

IN VITRO CYTOTOXICITY STUDY, SYNTHESIS AND SPECTROSCOPIC CHARACTERIZATION OF CR (III), PD (II), PT (IV) AND AU (III) HETEROCYCLIC LIGANDS COMPLEXES

Zinah N. Mahmood and Mahasin Alias*

Department of Chemistry, College of Science for Women, University of Baghdad, Baghdad, Iraq.

*e-mail: danaze888@yahoo.com

(Received 28 August 2019, Revised 19 November 2019, Accepted 27 November 2019)

ABSTRACT : New ligands derived from triazole derivatives and their complexes with metal ions Cr(III), Pd(II), Pt(IV) and Au(III) were prepared, in addition to Sodium fusidate complexes as (L_1), (L_2) and (L_3) respectively, these ligands were used to synthesize several new complexes by mixing with metal ions. All structures of these new compounds were rigorously characterized in the solid and solution states using spectroscopic techniques like: ^1H NMR, ^{13}C NMR, Uv-Vis, FTIR, metal and elemental analyses, magnetic susceptibility and conductivity measurements at room temperature, it was found that all ligands act as a bidentate chelate, and the geometry of the new complexes are identified as an octahedral geometry except (PdL_1 , AuL_1 & PdL_2) complexes which have square planar geometries. The biological activity of the ligands and their complexes as anticancer agents were evaluated *in vitro* using cis-Pt complex as control positive. The results obtained from cytotoxic assay, it can be concluded that the synthesized compounds are promising as new anticancer candidates in future especially in high concentration.

Key words : Spectroscopic techniques, bidentate chelate, *in vitro*, anticancer drugs.

INTRODUCTION

Many metal-containing compounds have been utilized throughout history to treat a wide variety of disorders. In medicinal chemistry—traditionally dominated by organic chemistry—metal complexes have gained favor as diagnostic tools and anticancer agents (Baile *et al*, 2015). Fusidic acid (FA), also known as sodium fusidate, is one of the hydrophobic antibiotics, and this compound which is used for the treatment of infections of sensitive osteomyelitis or skin and soft tissue caused by bacteria (Fernandes *et al*, 2016; Park *et al*, 2013; Steinkraus *et al*, 1979). Fusidic acid is clinically efficacious in combination with a variety of antibiotics (Whitby, 1999). This is due to the fact that the drug has shown low toxicity and bacterial resistance (Curbete and Salgado, 2016), which acts through the inhibition of bacterial protein synthesis (Magee *et al*, 2010) and it penetrates well into tissue and bone, it is often used for the treatment of *staphylococcal* osteomyelitis in conjunction with a second agent (Magee *et al*, 2010; Chen *et al*, 2017). FA is considered to be the most important member of the fusidane group (Curbete and Salgado, 2016), a small class of tetracyclic nor-triterpenes, they possess a cyclopentenoperhydrophenanthrene ring system and belong to the steroid class of compounds (Curbete and

Salgado, 2016). The compound having biological activity are most probably contain heterocyclic like quinolins, triazoles (Bhola *et al*, 2019) and Benzimidazole groups which exhibit a broad spectrum of biological activities, such as antifungal, antibacterial, antiviral, antitumor and antiparasitic activities (Zhang *et al*, 2012) especially 1,2,4-Triazole usually hold a series of pharmacological properties such as anticancer, antiviral, antitubercular, antifungal, and antibacterial activities (Zhang *et al*, 2012; Abdnor and Alabdali, 2019). Quinoline carboxylic acids and their analogues also show a wide variety of medicinal properties including antitumor, antiviral and estrogenic activity (Alias *et al*, 2015; Gobouri *et al*, 2019). In addition quinoline derivatives attract remarkable interest in coordination chemistry due to their coordination capability and also possess structural, chemical, electrochemical, photophysical, photochemical and catalytic properties (Fathima *et al*, 2019). The fact that few earlier conjugates of 1,2,4-triazole and quinoline, where these molecules are linked via oxygen- or amide-containing linkers in a single frame, are known to possess biological activities (Verbanac *et al*, 2016), the transition metal ions are responsible for proper functioning of different enzymes. The activity of bio metals is attained through the formation of complexes with different bio ligands and the mode of

biological action for complexes depends upon the thermodynamic and kinetic properties. The lipophilicity of the drug is increased through the formation of chelates and drug action is significantly increased due to effective permeability of the drug into the site of action (Baile *et al*, 2015).

MATERIALS AND METHODS

Sodium fusidate is a white, odorless, crystalline powder, sparingly soluble in water, Equipped by a company (SPAIN) purity (99.5%) and taken without further purification and all of the chemicals used in this work were analytical of highest purity available. All the products were characterized by CHNS elemental analysis, Resonance (NMR) spectroscopy, Ultraviolet-visible (Uv-Vis) spectroscopy, Fourier Transform Infrared FTIR Spectroscopy, Melting Point Determination, Magnetic Susceptibility and Molar Conductivity Measurements. The micro analytical data CHNS were collected using Euro EA3000, AA-680 Shimadzu Atomic Absorption Spectroscopy. ^1H and ^{13}C NMR spectrum was obtained using Bruker at 400MHZ employing DMSO d_6 solvent and as internal reference. FTIR spectra of the synthesized products were recorded using CsI disc using a Shimadzu and Perkin Elmer FTIR spectrometer. Electronic spectra of the ligands and their complexes in solution state were recorded on a Uv-Vis. 1800 PC Shimadzu Spectrophotometer. Magnetic Susceptibility Measurements of the complexes made by using Balance Johnson Matthey Catalytic System division at 25°C. The melting of all solid products was using Gallen Kamp M.F.B-60. The molar conductivity for the complexes in DMF solution. Optical density of each well in cell culture plates in cytotoxic assay was read by microELISA, at a transmitting wave length on 620 nm, plates of cell culture were incubated at 37°C in SANYO, incubator Japan.

Preparation of the ligands (L_2 & L_3)

Preparation of the 4-amino-5-(((5-methyl-1H-benzo[d]imidazol-2-yl)thio)methyl)-2,4-dihydro-3H-1,2,4-triazole-3-thiol (L_2)

This ligand (L_2) was prepared according to the general steps (Al-Dulimia *et al*, 2016; Nevade *et al*, 2013) supplied without further purification out lined in Scheme 1.

Synthesis of ethyl 2-((5-methyl-1H-benzo[d]imidazol-2-yl)thio)acetate (I)

A stirred mixture containing (4.5gm, 0.03 mole) of 2-mercapto-5-methylbenzimidazole, which dissolved in 60 ml of ethanol and (1.68gm, 0.03 mole) potassium hydroxide was added and heated at 78–80°C for 10 min,

then ethyl chloro acetate (3.66ml, 0.03 mole) was added in one portion an exothermic reaction set in causing a temperature rise from 30–40°C. After stirring at 25–30°C for 18 hrs. the reaction mixture was added to 100 gm of ice-water and stirred for 30 min at 0–10°C. The precipitate was collected by filtration, washed with water until free of chloride and dried in air at 50°C, then recrystallized by ethanol.

Synthesis of 2-((5-methyl-1H-benzo[d]imidazol-2-yl)thio)acetohydrazide (II)

The mixture of compound (I) (4 gm, 0.004 mole) and Hydrazine hydrate (6 ml, 0.01 mole) are mixed well in a round butyl flask and heated on water bath at (78–80) °C for 10 min, then dissolved in 60 ml ethanol. The reaction mixture was heated with reflux condenser for six hours, cooled to room temperature and the reaction mixture was added to 100 gm of ice-water, and kept aside for crystallization. The colorless crystals are collected by filtration, and recrystallized from ethanol.

Synthesis of 2-(2-((5-methyl-1H-benzo[d]imidazol-2-yl)thio)acetyl)hydrazine-1-carbodithioic acid, potassium salt(III)

To continuously stirred solution of potassium hydroxide (2.565 g, 0.015 mole) and compound II in absolute dry ethanol (100 ml), carbon disulphide (2.7 ml, 0.015 mole) was added dropwise. After the complete addition the mixture was diluted by 75 ml of absolute ethanol and agitated for 16 hrs. Then diluted with dry ether (100 ml) and the solid precipitates was collected by filtration, washed with dry ether at 65°C and then obtained crude suspension of potassium dithiocarbonate.

Synthesis of 4-amino-5-(((5-methyl-1H-benzo[d]imidazol-2-yl)thio)methyl)-4H-1,2,4-triazole-3-thiol (L_2)

To above suspension hydrazine hydrate (1.86 ml, 0.02 mole) was added and the mixture was reflux for 2 hrs. the color of mixture reaction changed to green with the volatilize of hydrogen sulphide gas and homogeneous mass was obtained, then cooled and diluted with 100 ml of cold water. The cold mixture was acidified with concentrated hydrochloric acid. The solid separated was filtered, washed with the water, dried and recrystallized from water.

Preparation of the 4-amino-5-(quinolin-2-yl)-4H-1,2,4-triazole-3-thiol (L_3)

The ligand (L_3) was prepared starting from 2-Carboxy quinoline (2Q) according to the following general steps (Al-Dulimia *et al*, 2016; Nevade *et al*, 2013) can be seen in Scheme 2.

Synthesis of methyl quinoline-2-carboxylate (I)

Sulphuric acid (8 ml) was added dropwise with continuous stirring to a solution of 2-Carboxy quinoline (2Q)(1.73g) in absolute ethanol. The mixture was heated under reflux for 10 hrs., after cooling, the mixture was poured on to crush ice; the precipitated crystalline solid was filtered, washed successively with water, 10% NaHCO_3 solution and water. The crude product was recrystallized from ethanol to give compound (I) as off-white crystals.

Synthesis of quinoline-2-carbohydrazide (II)

Ester of (I) (1.87g, 0.01 mol) was dissolved in absolute ethanol (50 ml). To the above solution was added 80 % hydrazine hydrate (0.1 mol). The resulting reaction mixture was refluxed on a steam bath for 10-12 hrs. After cooling, 150 ml of cold water was added to the mixture and the separated white crystalline solid was filtered, washed with cold water, dried and recrystallized from ethanol.

Synthesis of potassium 2-(quinoline-2-carbonyl)hydrazine-1-carbodithioate(III)

Compound (II) (0.935g, 0.005 mol) was treated with a solution of potassium hydroxide (0.0643 mol) in (70 ml) ethanol at 0°C with stirring, then 7 ml of carbon disulfide was added dropwise and the reaction mixture was stirred overnight at room temperature. The solid product (III) was filtered, washed with cold methanol and dried.

Synthesis of 4-amino-5-(quinolin-2-yl)-4H-1,2,4-triazole-3-thiol (L_3)

A mixture of compound (III) (1.495g, 0.005 mol) and 80 % hydrazine hydrate (10 ml) was heated under reflux till the volatilize of hydrogen sulphide completely ceases (about 6 hrs.), after cooling 200 ml of water was added and the mixture was neutralized with 10% HCl and allowed to stand for three hours. The separated crude product was filtered, washed with water, dried and recrystallized from ethanol.

Synthesis of Metal complexes

General procedure to prepare some complexes of ligand (L_1)

A solid salts of $[\text{CrCl}_3 \cdot 6\text{H}_2\text{O}]$ (0.266 gm), $\text{H}_2\text{PtCl}_6 \cdot 6\text{H}_2\text{O}$ (0.517 gm), PdCl_2 (0.177 gm) and $\text{HAuCl}_4 \cdot \text{H}_2\text{O}$ (0.357 gm)] dissolved in ethanol was added to 10 ml of ethanolic solution for L_1 with stirring in (1:2) molar ratio. The mixture was heated under reflux for 3 hrs. during this time a precipitate was formed then filtered, washed several times with water to in order remove the NaCl and then dried under vacuum and crystallized from ethanol. All prepared complexes were identified using

spectroscopy, analytical and physical measurements.

General procedure to prepare some complexes of (L_2) & (L_3)

The present mixed complexes of (L_2 & L_3) were prepared by mixing of (L_2) dissolved in 10 ml of absolute ethanol with metal salt of $[\text{CrCl}_3 \cdot 6\text{H}_2\text{O}]$ (0.266 gm), $\text{H}_2\text{PtCl}_6 \cdot 6\text{H}_2\text{O}$ (0.517 gm) PdCl_2 (0.177 gm) and $\text{HAuCl}_4 \cdot \text{H}_2\text{O}$ (0.357 gm)] which dissolved in 5 ml of absolute ethanol, and the same way and ratio was used to prepare the new complexes of L_3 . The mixture was heated under reflux for 2-3 hrs. during this time a precipitate was formed which was filtered and crystallized from ethanol then dried under vacuum at 60°C . All prepared complexes were identified using spectroscopy, analytical and physical measurements.

Formation of Metal complexes for (L_1 , L_2 & L_3) in Solution state

The formation of complexes in solution state was studied for L_1 , L_2 & L_3 with Cr(III), Pt(IV), Pd(II) and Au(III) using ethanol as a solvent and molar ratio method, in order to determined M: L ratio. In this study, the molar ratio plot was obtained by adding an increased amount of ligand (0.25-5.00 ml) of 10^{-3}M to a constant amount of metal ion (1 ml) of 10^{-3}M in a final volume of (10 ml) absolute ethanol (Skooge *et al*, 2014). From relationship between the absorption of the absorbed light and the molar ratio of M:L at λ_{max} the M:L ratio was determined. The absorbance (A_s and A_m) of the solution have been measured at λ_{max} of maximum absorption. The stability constant (K) (eq.1) and the molar absorptivity (ϵ_{max}) (eq. 2) were calculated using the following equations :

$$K = \frac{1 - \alpha}{4\alpha^3 C^2} \quad (1)$$

When, M:L is (1:2)

$$A_m = \epsilon_{\text{max}} bc \quad (2)$$

Where,

A_m = Absorbance of the solution containing an excess constant amount of ligand.

A_s = Absorbance of the solution containing stoichiometric amount of ligand metal ion.

b = Cell constant ($b = 1\text{cm}$).

c = Molar concentration.

Cytotoxic assay

The cytotoxic effect of the prepared compounds was determined using the colometric 3-(4,5-dimethyl thiazole-2-yl)-2,5-biphenyl tetrazolium bromide(MTT) assay.

MDA-231 cell lines was used in this study were equipped from biotechnology center/Al-Nahrain University, the cell were grown in Minimum Essential Medium (MEM) with 10% fetal bovine serum, (100U/ml) of penicillin and (100mg) of streptomycin/ml in a humidified incubator with (5% CO₂) at (37°C). Briefly, cells were seeded in 96-well microtiter plates. After exposure to various concentrations of compounds as well as control positive (cis-Pt) (400, 200, 100, 50 & 25 µg/ml) for 48 hr. cells were washed once with phosphate-buffered saline (PBS) before addition of 100 µl of serum free medium containing 5 mg/ml of MTT to each well, the mixture was absorbance was read at 620 nm. The Statistical Analysis System- (SAS, 2012) Version 9.1th ed. program was used to detect the effect of difference concentration in Inhibition rate. Least significant difference–LSD test (Analysis of Variation-ANOVA- One way) was used to significant compare between means in this study.

RESULTS AND DISCUSSION

The obtained complexes were colored powders stable for a long time in the open atmosphere. The analytical data for the ligands and their complexes together with some physical properties are summarized in Table 1. All complexes were soluble in general organic solvents, to confirm the molar ratio between metal complexes, at the maximum absorption, absorbance A_s and A_m of the solution were measured at a maximum wavelength. The stability constant K and molar absorptive ε_{max} have been also calculated. The data of complexes formation can be listed in Table 2.

FT-IR spectra

The FTIR spectra provide valuable interaction regarding the nature of the functional group attached to metal ion. The characteristic frequencies of free ligands and their metal complexes have been readily assigned in comparison with the literature values (Nakamoto, 2009). The infrared bands of L₁ shown sharp and medium characteristic absorption bands which occurred at 1550 and 1388 cm⁻¹ due to stretching asymmetric and symmetric ν COO⁻ respectively and the change in the frequency Δν was equal to 162 cm⁻¹, also showed three bands at (3487, 3417, 1712 & 1269) cm⁻¹ were caused by vibration of hydrogen bonded and carboxyl ester groups. The IR spectra of the complexes observed Δν(COO⁻) are very useful in describing structure of the prepared compounds. The ν_{asym}(COO⁻) stretching appeared in range of (1530-1523) cm⁻¹ while vibration observed in the range of (1377-1371) cm⁻¹

Table 1 : The physical properties, elemental and metal content for all compounds.

Comp.	Color	M.Wt g/mol	m.p °C	Yield %	Molar ratio (M:L)	Elemental analysis found (Calc.)				Metal % found (Calc.)	Molecular Formula
						C	H	N	S		
L ₁	White	538.7	204-206d	—	—	(69.05)	(8.72)	—	—	—	C ₃₁ H ₄₇ NaO ₆
CrL ₁	Green	1144.5	160-162	66	1:2	64.67(65.00)	8.23(8.47)	—	—	4.31(4.54)	CrC ₆₂ H ₉₇ O _{13.5} Cl
PdL ₁	Brown	1136.4	158-160	80	1:2	65.12(65.46)	7.81(8.27)	—	—	8.64(9.36)	PdC ₆₂ H ₉₄ O ₁₂
PtL ₁	Yellow	1305.0	138-140	83	1:2	55.98(57.01)	6.89(7.27)	—	—	13.56(14.94)	PtC ₆₂ H ₉₅ O _{12.5} Cl ₂
AuL ₁	Yellowishbrown	1271.5	100-102	88	1:2	57.87(58.51)	7.11(7.47)	—	—	14.94(15.49)	AuC ₆₂ H ₉₅ O _{12.5} Cl
L ₂	Beige	292.0	256-258d	61	—	45.01(45.20)	3.85(4.10)	28.18(28.76)	21.47(21.91)	—	C ₁₁ H ₁₂ N ₆ S ₂
CrL ₂	Green	705.5	220d	72	1:2	37.08(37.42)	3.21(3.68)	23.11(23.81)	17.54(18.14)	6.72(7.37)	CrC ₂₂ H ₂₆ N ₁₂ S ₂ O ₂ Cl
PdL ₂	Brown	734.4	224-226	82	1:2	38.77(39.21)	3.05(3.81)	22.17(22.87)	16.37(17.42)	13.68(14.48)	PdC ₂₄ H ₂₈ N ₁₂ S ₄ O
PtL ₂	Reddishbrown	866.0	214-216	77	1:2	29.58(30.48)	2.27(2.77)	18.84(19.39)	14.26(14.78)	21.37(22.51)	PtC ₂₂ H ₂₄ N ₁₂ S ₄ OCl ₂
AuL ₂	Dark brown	878.5	222-224d	69	1:2	32.11(32.78)	2.91(3.41)	18.55(19.12)	13.83(14.57)	21.82(22.42)	AuC ₂₄ H ₃₀ N ₁₂ S ₄ OCl
L ₃	Beige	243.0	254-256d	56	—	53.77(54.32)	3.11(3.70)	28.31(28.80)	13.02(13.16)	—	C ₁₁ H ₉ N ₅ S
CrL ₃	Green	607.5	230-232d	77	1:2	43.01(43.45)	2.91(3.29)	22.65(23.04)	9.82(10.53)	8.04(8.55)	CrC ₂₂ H ₂₂ N ₁₀ S ₂ O ₂ Cl
AuL ₃	Dark brown	780.5	224-226d	72	1:2	36.17(36.89)	2.64(3.07)	16.93(17.93)	7.52(8.19)	24.45(25.24)	AuC ₂₄ H ₂₄ N ₁₀ S ₂ O ₂ Cl

d : decomposition degree

Table 2 : Stability constant and molar absorptivity for all prepared complexes at room temperature.

Comp.	A_s	A_m	ϵ	$\epsilon_{\max} \text{ L.mol}^{-1} \text{ cm}^{-1}$	$K \text{ L}^2 \text{ mol}^{-2}$	$\lambda_{\max} \text{ (nm)}$
CrL ₁	0.25	0.35	0.285	3500	7.65×10^6	420
PdL ₁	0.71	0.82	0.134	8200	8.96×10^7	414
PtL ₁	1.06	1.14	0.070	11400	6.73×10^8	377
AuL ₁	0.077	0.085	0.094	850	2.72×10^8	370
CrL ₂	0.29	0.41	0.292	4100	7.05×10^6	416
PdL ₂	0.48	0.59	0.186	5900	3.13×10^7	420
PtL ₂	0.93	1.01	0.079	10100	4.63×10^8	380
AuL ₂	0.81	0.95	0.147	9500	6.66×10^7	385
CrL ₃	0.021	0.029	0.275	290	8.62×10^6	424
AuL ₃	0.81	0.89	0.089	8900	3.13×10^8	390

K = Stability constant obtained as the average of three measurements.

As : Average of three measurements of the absorption of the solution containing a stoichiometric amount of ligand and metal ion. Am: Average of three measurements of the absorption of solution containing the same amount of metal and five fold excess of ligand.

are $\nu_{\text{sym}}(\text{COO}^-)$, the difference $\Delta \nu(\text{COO}^-)$ propose a bidentate coordination, which $\Delta \nu$ value come out to be less than ionic compound (Xiao *et al.*, 2019) as shown in Table 3. More evidences of new medium or weak bands which appeared in prepared complexes, this attributed to the $\nu(\text{M-O})$ and $\nu(\text{M-Cl})$ in the range (559-528) and (320-312) cm^{-1} respectively. A broad peak which appears in the range (3582-3310) cm^{-1} which refer to presence ethanol or/and water molecules in the sphere coordinated or out of sphere. And other bands for Cr complex appeared at (918) and (848) cm^{-1} is due to rocking and wagging $\delta \text{H}_2\text{O}$ indicating the presence of water within the field of coordination (Nakamoto, 2009; Xiao *et al.*, 2019; Deacon and Phillips, 1980). Other bands are shown in Table 3.

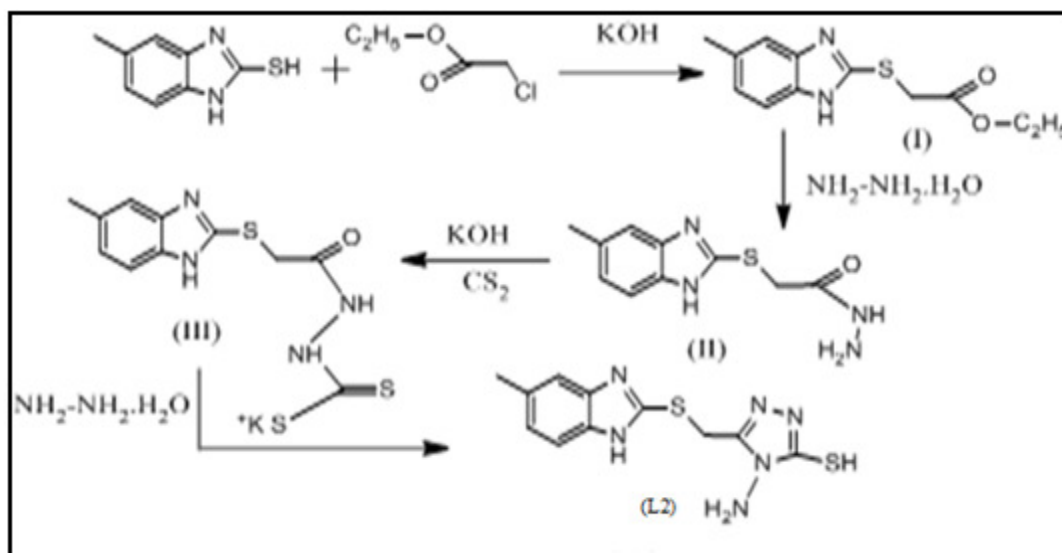
The ligand (L_2) was determined by FTIR spectroscopy for the free ligand and its complexes and their probable assignment are given in Table 3. This ligand contain thioamide groups ($-\text{N}=\text{C}-\text{SH}$ or $\text{H}-\text{N}=\text{C}=\text{S}$) (Symal and Bari, 1984; Alias *et al.*, 2008) and nitrogen of the azomethine group and displays distinct $\nu(\text{S-H})$ at (2573 cm^{-1}) and $\nu(\text{N-H})$ at (3130, 3030 and 2981) cm^{-1} due to strong hydrogen bonding vibrations indicative of both thiol and thion groups. These two bands disappeared in the spectra of the metal complexes, the NH band shifted to lower frequency for the originally band (3130 cm^{-1}), and the two peaks at 3030 and 2981 cm^{-1} of the ligand. This is more indicated by observing thioamide band (I) which is due to ($\delta \text{NH} + \nu \text{C}=\text{C}$) major, this band disappeared in the spectra of metals complexes. The IR spectra of the complexes in Table (3) showed medium to strong bands at (1597, 1357, 975 and 744) cm^{-1} which may be assigned to thioamide vibrational bands (I-IV), respectively (Abdulla *et al.*, 2007). This behavior has been previously reported for other metal complexes of heterocyclic thiols (Scozzafava *et al.*, 1998). Thioamide

band (II) was shifted to higher frequency of metals compounds, this indicate the involvement of the N of the SCN moiety in coordination with the metal or some other time this band splitting to two weak bands one of them shifted to the high frequency and other to lower frequency (Mishra *et al.*, 2019). The involvement of S-atom in the coordination is indicated by nearly disappearance of thioamide band (III) which has major contribution from $\text{C}=\text{S}$ frequency (Mishra *et al.*, 2019). The coordination of both (N, S) atoms to the metal is further indicated by the observation that the band (IV) did not change in position, and more supported for this proposed coordination, there is new weak band which appear in the region (551-532) and (470-466) cm^{-1} which refer to M-N and M-S band stretching (Alias, 2007). The IR spectral observation reveal that chromium ion was bonded to triazole moiety through both S and N atoms, as a bidentate ligand while heavy metals, when the triazole contains an (S-C-N-N) unite that allows for bidentate coordination through the nitrogen of amine and sulphur of thiocarbonyl group to form stable five membered ring (Al-Maydama *et al.*, 2008). Other bands in the spectra of these compounds can be display in Table 3.

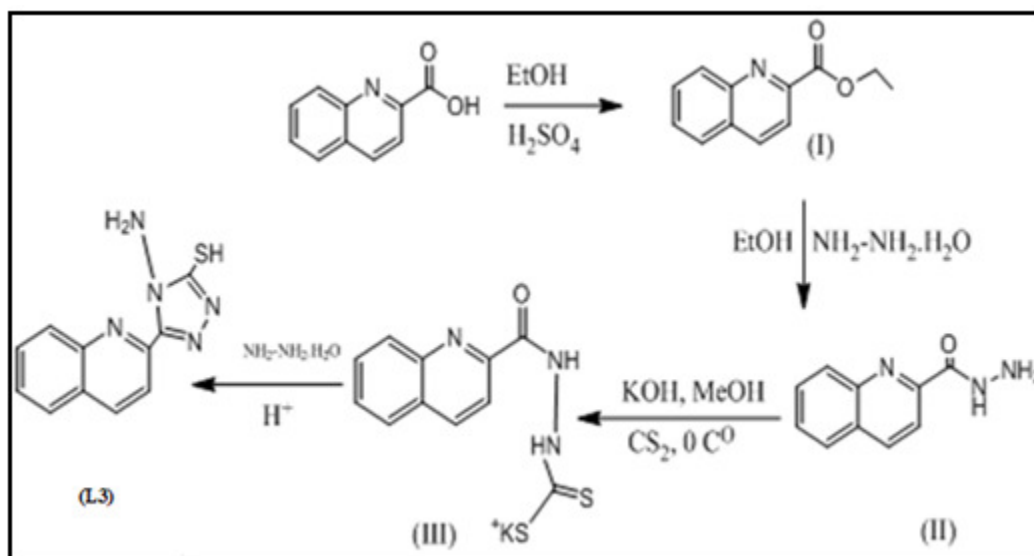
Ligand (L_3) displays distinct $\nu(\text{S-H})$ at 2573 cm^{-1} and $\nu(\text{N-H})$ at 3130, 3030 and 2981 cm^{-1} due to strong hydrogen bonding vibrations indicative of both thiol and thion groups. These two bands disappeared in the spectra of the metal complexes, the NH band shifted to lower frequency for the originally band (3130 cm^{-1}) and the two peaks at 3030 and 2981 cm^{-1} of the ligand. This is more indicated by observing thioamide band (I), which is due to ($\delta \text{NH} + \nu \text{C}=\text{C}$) major, this band disappeared in the spectra of metals complexes. The IR spectra of the complexes in Table 3 showed medium to strong bands at (1597, 1296, 964 and 763 cm^{-1}) which may be assigned to thioamide vibrational bands (I-IV) respectively (Alias,

Table 3 : FTIR absorption data for ligands and their metal complexes.

Formal	ν OH	ν NH ₂ Asym.Sym.	ν SH	ν C=O (aster)	ν COO ⁻ (asym.)(sym.)	ν C-OH	Thioamide I ν NH+ ν C=C	Thioamide II ν C=N+ ν C=C	Thioamide III ν N-C-S	Thioamide IV ν C-S	Others
L1	3487, 3417	—	—	1712	1550 1388	1269	—	—	—	—	—
CrL1	3410	—	—	1712	1523 1377	1265	—	—	—	—	ν H ₂ O = 3582 -3379 ω H ₂ O=918, ρ H ₂ O=848, ν Cr-Cl=312
PdL ₁	3487, 3417	—	—	1716	1529 1377	1261	—	—	—	—	—
PtL1	3468, 3414	—	—	1716	1529 1371	1261	—	—	—	—	ν H ₂ O= 3570 -3310 ν Pt-Cl=320
AuL1	3480, 3414	—	—	1712	1530 1377	1265	—	—	—	—	ν H ₂ O= 3570 -3360
L ₂	—	3270 3200	2573	—	—	—	1597, 1547	1357	975m.	744	—
CrL2	—	3273 3204	—	—	—	—	1608, 1562	1396 1311	970 v.w.	740	ν H ₂ O=3486a H ₂ O=905, ρ H ₂ O=8795 ν Cr-Cl= 324
PdL ₂	—	32 77	—	—	—	—	1616, 1598, 1549	1418 1340	963 v.w.	737	ν EtOH = 3410
PtL2	—	3278	—	—	—	—	1616, 1560	1400 1360	964 v.w.	736	ν H ₂ O = 3440 ν Pt-Cl= 308
AuL2	—	3437, 3394, 3270	—	—	—	—	1624, 1599, 1548, 1508	1420, 1367	963v.w.	736	ν EtOH = 3520 -3480a H ₂ O= 921 ρ H ₂ O=8585 ν Au-Cl= 320
L3	—	3270 3200	2584	—	—	—	1625 1597 1543	1296	964	763	—
CrL3	—	3275 3200	—	—	—	—	1610 1538	1384 1285	964v.w.	759	ν H ₂ O=3410 ω H ₂ O=934 $\bar{\nu}$ H ₂ O=8795 ν Cr-Cl=312
AuL3	—	3260 3155	—	—	—	—	1600 1550 1516	1388	979 v.w.	752	ν H ₂ O=3402 H ₂ O=952 $\bar{\nu}$ H ₂ O=8795 ν Au-Cl=329



Scheme 1 : General steps of prepared 4-amino-5-(((5-methyl-1H-benzo[d]imidazol-2-yl)thio)methyl)-2,4-dihydro-3H-1,2,4-triazole-3-thiol (L₂).



Scheme 2 : General steps of prepared of 4-amino-5-(quinolin-2-yl)-4H-1,2,4-triazole-3-thiol(L₃).

2007). This behavior has been previously reported for other metal complexes of heterocyclic thiols (Abdulla *et al*, 2007). Thioamide band (II) was shifted to higher frequency of metals compounds about (1388) cm⁻¹. The involvement of S-atom in the coordination is indicated by nearly disappearance of thioamide band (III) which has major contribution from C=S.

The coordination of both N and S atoms to the metal is further indicated by the observation that the band (IV) did not change in position. More exhibited there is new weak bands which appear in the range (563-443 cm⁻¹) which refer to M-N and M-S band stretching (Alias, 2007). The IR spectral observation reveals that the chromium ion was bonded to triazole moiety through both S and N atoms, as a bidentate ligand while gold complexes which coordinate with triazole through (S-C-

N-N) group that allows for bidentate coordination through the nitrogen of amine and sulphur of thiocarbonyl group to form a stable five-membered ring (Al-Maydama *et al*, 2008). More evidence there is new weak bands which appear in the range (563-540) and (455-443) cm⁻¹ which refer to M-N and M-S stretching bands.

Magnetic moments, electronic spectral data and conductivity measurements

The electronic spectrum of free ligand (L₁) exhibited three main bands. The first absorption band appeared at 225 nm due to interligand transition ($\delta \rightarrow \delta^*$) located on the pi-system. The second absorption band located at 242 nm also arises from ($\delta \rightarrow \delta^*$) transition but within another group. The third absorption band is attributed to ($n \rightarrow \delta^*$) electronic transition located on the oxygen atoms (carboxylate, ester and OH) which appeared at 270 nm.

Table 4 : Electronic spectra, conductance in DMF solvent and magnetic moment (B.M) for the prepared ligands and their metal complexes.

Formula	Absorption cm^{-1}	Assignments	B°	$B2$	β	$\frac{Dq}{B'}$	$10Dq$	$15B2$	μ_{eff} B.M	Conductivity S cm^{-1}	Suggested geometry
L1	3703 741322 44444	$n \rightarrow \pi^*$ $\pi \rightarrow \pi^*$	—	—	—	—	—	—	—	—	—
CrL1	15873 23809 34482 34313(cal.)	$^4A_2g \rightarrow ^4T_2g$ $^4A_1g \rightarrow ^4T_1g$ $L \rightarrow \text{Cr CT}$	918	700.2	0.762	2.25	15754	10533	3.21	22	Octahedral distortion
PdL1	24154 26246 31746	$^1A_1g \rightarrow ^1B_1g$ $g^1A_1g \rightarrow ^1Eg$ $L \rightarrow \text{Pd CT}$	—	—	—	—	—	—	—	30	Square planar
PtL1	9960 26525 37037 45454	$^1A_1g \rightarrow ^3T_1g$, $^3T_2g^1A_1g \rightarrow ^1T_2g$ $g^1A_1g \rightarrow ^1T_1g$ $L \rightarrow \text{Pt CT}$	—	—	—	—	—	—	0.012	26	Octahedral distortion
AuL1	27027 34482	$^1A_1g \rightarrow ^1B_1g^1$ $A_1g \rightarrow ^1Eg$	—	—	—	—	—	—	0.00	74	Square planar
L2	30303 38461 42016	$n \rightarrow \pi^*$ $\pi \rightarrow \pi^*$	—	—	—	—	—	—	—	—	—
CrL2	15723 24875 33333 33257(cal.)	$^4A_2g \rightarrow ^4T_2g^4$ $A_1g \rightarrow ^4T_1g$ $L \rightarrow \text{Cr CT}$	918	730.9	0.796	2.15	15695	10963.5	3.36	12	Octahedral distortion
PdL2	23809 32258 35460	$^1A_1g \rightarrow ^1B_1g$ $^1A_1g \rightarrow ^1Eg$ $L \rightarrow \text{Cr CT}$	—	—	—	—	—	—	—	31	Square planar
PtL2	10030 26315 35087 39215	$^1A_1g \rightarrow ^3T_1g$, $^3T_2g^1A_1g \rightarrow ^1T_2g^1$ $A_1g \rightarrow ^1T_1g$ $L \rightarrow \text{Pt CT}$	—	—	—	—	—	—	0.008	20	Octahedral distortion
AuL2	25974 28985 57089(cal.) 40816	$^3A_1g \rightarrow ^3T_2g^3$ $A_1g \rightarrow ^3T_1g$ $g^3A_1g \rightarrow ^3T_1g(p)$ $L \rightarrow \text{Au CT}$	—	896	—	2.70	24210	13440	2.66	25	Octahedral distortion
L3	25000 31250 40816 42735	$n \rightarrow \pi^*$	—	—	—	—	—	—	—	—	—
CrL3	16077 24570 35087 35052(cal.)	$^4A_2g \rightarrow ^4T_2g^4$ $A_1g \rightarrow ^4T_1g$ $L \rightarrow \text{Cr CT}$	918	759.4	0.827	2.1	15947	11391.75	3.27	16	Octahedral distortion
AuL3	25641 30303 59811(cal.) 34602 37735	$^3A_1g \rightarrow ^3T_2g^3$ $A_1g \rightarrow ^3T_1g$ $^3A_1g \rightarrow ^3T_1g(p)$ $L \rightarrow \text{Au CT}$ $L \rightarrow \text{Au CT}$	—	886.6	—	2.89	25605	13299	2.54	23	Octahedral distortion

(Lotfy *et al*, 2015).

The electronic spectra of free ligands (L_2 and L_3) appeared also three absorption bands. The first and second absorption exhibited at 238, 260 and 234,245 nm

respectively, corresponding to ($\delta \rightarrow \delta^*$) transition, the third band attributed to the ($n \rightarrow \delta^*$) transition at 330 and 320, 400nm respectively refer to donor atom of S and N atom in $C = N$ group (Joshi *et al*, 2019).

Table 5 : ¹HNMR spectra data of ligands and their metal complexes.

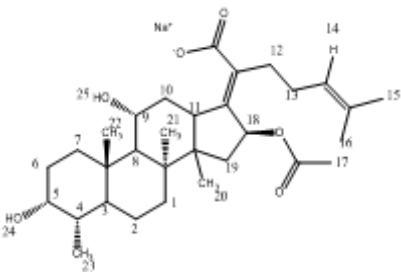
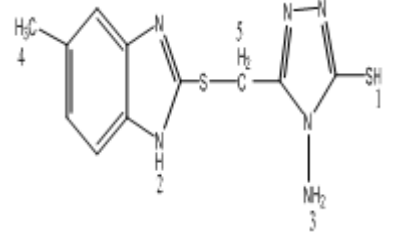
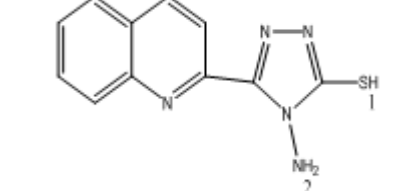
Ligands	¹ HNMR
	L1: ¹ HNMR(DMSO- d ₆)δ ppmä 0.83-0.93 ppm (s,3H,H ₂₀ -H ₂₂ and d,3H,H ₂₃) (CH ₃ cyclic of L ₁), ä 1.03-1.93ppm to (s,H ₁ -H ₁₀) ppm except peaks in the range ä 3.51-3.59 as (s,H ₅ and H ₉)ppm to protonon (-CH-OH) groups. Also shows signal as peaks in ä 1.75 and 1.88 ppm to aliphatic methyl proton ⁽¹⁾ as a ä 1.75(s,3H,H ₁₆) and ä 1.88(s,3H,H ₁₅)ppm. Also shows at ä 2.07(s, H ₁₂ and H ₁₃)ppm to aliphatic methylene (CH ₂ -CH ₂) proton ^(2,1) , and at ä 5.30-5.35(t,H,H ₁₄ ,H ₁₈)ppm. The peaks on ä 2.26 and 2.28(s, 1H, H ₁₇)ppm which is ascribed aliphatic methyl on ester group (CH ₃ -COO-) proton, and peak which appeared on ä 4.28-4.30ppm which corresponding to proton on (-OH) group.The comparison of ¹ HNMR spectra of Pd(II), Pt(IV) andAu (III) complexes formed with the ligand spectrum position of proton aboutconfirming the coordination, a very little shifting in the proton position of the ligand with these metal complexes
	L2: ¹ HNMR(DMSO- d ₆)δ ppmäSH=13.78ppm (s,H, SH) of thiol groupäNH ₂ =5.64ppm (s, 2H, NH ₂) of amine groupäNH=12.46ppm (s, H, NH) of binzimidazole groupäCH ₂ =4.64ppm (s, 2H, CH ₂) of methylene groupäCH ₃ =2.79ppm(s, 1H, NH)of CH ₃ groupäPh =7.11-7.40ppm of phenyl group (3H)The comparison of ¹ HNMR spectra of Pd(II) and Pt(IV) complexes formed with the ligand spectrum the absorption peak of the proton SH group was disappearedand exhibits some shift in the position of proton NH ₂ about 5.10and 5.08 ppm forPd(II) and Pt(IV) complexes respectively, this confirming that these moieties(NH ₂ and SH) coordination with two metal complexes
	L3: ¹ HNMR(DMSO- d ₆)δ ppmäSH=13.80ppm (s,H, SH) of thiol groupäNH ₂ =5.91ppm(s, 2H, NH ₂) of amine groupäPh =6.67-8.61ppm of phenyl group (5H)The comparison of ¹ HNMR spectra of Cr(III) complex formed with the ligand spectrum exhibits disappearance the proton of thiol absorption peak and shifting in the absorption peak of amine group about ä 13.78 ppm confirming the coordination moiety of the ligand (SH and NH2) with metal complex

Table 6 : ¹³CNMR spectra data of ligands and their metal complexes.

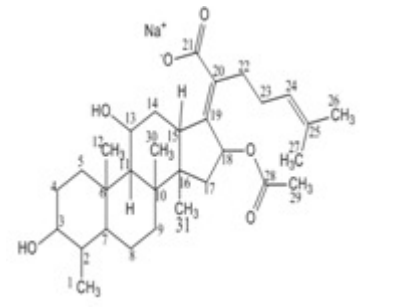
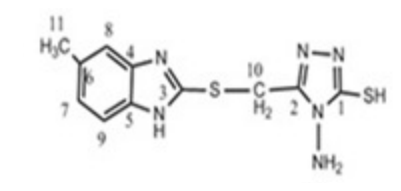
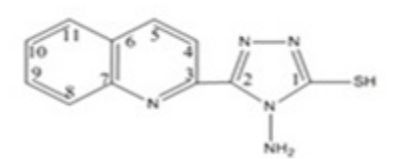
Ligands	¹³ CNMR
	L1: ¹³ CNMR(DMSO-d ₆)äppm15.51 (C ₁ and C ₁₂ CH ₃ cyclic of sodium fusidate), 18.74 (C ₃₀ and C ₃₁ CH ₃ cyclic of ligand (L1),22.14 and 24.94 (C ₂₆ ,C ₂₇ and C ₂₉ CH ₃ - aliphatic),28.74,29.69 (C ₂₂ and C ₂₃ CH ₂ - CH ₂ aliphatic), 31.29-35.80 (C ₄ , C ₅ ,C ₉ ,C ₁₄ and C ₁₅ CH ₂ - cyclic of ligand (L1), 41.94 and 42.14 (C ₂ and C ₆ CH- cyclic of ligand (L1),45.66 (C ₁₀ ,and C ₁₇), 48.14(C ₇ ,and C ₁₆ C- cyclic of ligand (L1), 55.71(C ₁₁), 68.15(C ₁₃ , C-OH), 77.75 and 78.94(C ₃ and C ₁₈ C-OH), 125.55 and 132.21 (C ₂₄ and C ₂₅ CH=C(CH ₃) ₂), 139.51 (C ₂₀ C=C), 170.75 and 171.94 (C ₂₁ and C ₂₈ COO carboxyl).The comparison of ¹³ CNMR spectra of Pd(II), Pt(IV) andAu (III) complexes formed with the ligand spectrum. There is shifting in the peak of C=C group to ä 165.52- 165.61ppm, and the peak of COO to ä 178.78- 179.14ppm group in the ligand with these metal complexes this is confirming the coordination compounds.
	L2: ¹³ CNMR(DMSO-d ₆)äppm167.59(C ₁), 153.51(C ₂), 150.01(C ₃),139.33(C ₄) 136.71(C ₅),133.73(C ₆), 126.74(C ₇),118.14(C ₈ and C ₉) 31.71(C ₁₀) and 22.74(C ₁₁)The comparison of ¹³ CNMR spectra ofPd(II) and Pt(IV) complexes formed position of carbon atoms confirming coordination compoundsandthe shifting in the peak of C ₁ in C-SH in trizole to ä 160.50- 160.61ppm for all complexes
	L3: ¹³ CNMR(DMSO-d ₆)äppm170.59(C ₁), 147.71(C ₂), 159.51(C ₃), 120.20(C ₄)138.22(C ₅), 145.51(C ₆), 126.62(C ₇), 121.11(C ₈),131.19(C ₉), 128.52(C ₁₀) and 129.92(C ₁₁)The comparison of ¹³ CNMR spectra of Cr(II) complex formed position of carbon atoms confirming the coordination this compound and the shifting in the absorption peak of C1 in trizole to ä 161.69ppm for the metal complex

Table 7 : Statistical data and IC_{50} values of L_1 and its metal complexes as well as control positive on MDA-231 cells lines in time of exposure 48 hrs.

Conc.	Inhibition rate% (means \pm standard deviation \pm SD)						
	Cis Pt	L1	CrL1	PdL1	PtL1	AuL1	LSD value
400	73.78 \pm 1.08aDE	70.96 \pm 0.97aE	77.33 \pm 1.03aCD	89.62 \pm 0.58aA	81.04 \pm 1.51aBC	84.01 \pm 1.17aB	4.537 *
200	61.91 \pm 1.11bB	59.19 \pm 1.66bB	62.50 \pm 1.96bB	70.08 \pm 1.37 bA	50.57 \pm 0.24bC	60.99 \pm 0.59bB	4.025 *
100	51.00 \pm 1.12cA	53.97 \pm 1.04cA	39.01 \pm 0.94cCD	34.84 \pm 0.89cD	43.64 \pm 1.09cC	40.69 \pm 0.78cC	5.483 *
50	46.09 \pm 0.69dA	42.93 \pm 1.68dA	35.89 \pm 1.17dB	27.22 \pm 1.55 dD	33.47 \pm 1.04dBC	29.16 \pm 1.58dCD	5.194 *
25	32.89 \pm 1.68eB	39.89 \pm 1.84eA	30.00 \pm 2.48eB	20.75 \pm 1.27eC	28.77 \pm 0.97eB	22.49 \pm 2.33eC	4.377 *
LSD value	2.149 *	2.698 *	2.970 *	2.163 *	1.921 *	2.612 *	—
IC_{50}	41.77	43.87	33.97	27.56	32.12	29.09	—

Means having with the different letters in same column differed significantly, * (P<0.05).

Table 8 : Statistical data and IC_{50} Values of L_2 and its metal complexes as well as control positive on MDA-231 cells lines in time of exposure 48 hrs.

Conc.	Inhibition rate% (means \pm standard deviation \pm SD)						
	Cis –platin	Ligand 2	CrL2	PdL2	PtL2	AuL2	LSD value
400	73.78 \pm 1.08aD	68.98 \pm 1.55aD	78.50 \pm 1.07aC	87.91 \pm 0.27a A	80.08 \pm 1.25a BC	84.89 \pm 0.63a AB	4.189*
200	61.91 \pm 1.11bBC	64.89 \pm 1.03bAB	55.32 \pm 1.03bDE	50.33 \pm 2.16bE	58.01 \pm 1.29bCD	68.33 \pm 1.44bA	5.442*
100	51.00 \pm 1.12cB	59.93 \pm 1.56cA	50.16 \pm 1.76cB	46.10 \pm 0.41cBC	43.86 \pm 1.74cCD	39.88 \pm 1.27cD	5.621*
50	46.09 \pm 0.69dA	50.97 \pm 2.07dA	37.36 \pm 1.55dB	31.98 \pm 1.06dC	39.98 \pm 1.35dB	34.98 \pm 1.25dBC	5.084*
25	32.89 \pm 1.68eB	39.98 \pm 1.71eA	29.31 \pm 1.09eBC	20.20 \pm 0.52eE	25.05 \pm 1.42eCD	23.83 \pm 1.14eDE	4.314*
LSD value	2.149 *	2.951 *	2.435 *	2.050 *	2.592 *	2.100 *	—
IC_{50}	41.77	49.03	36.12	29.03	34.07	32.32	—

Means having with the different letters in same column differed significantly, * (P<0.05).

CrL₁, CrL₂ and CrL₃

The ν_1 and ν_2 transition are spin allowed and laporte forbidden which corresponding to $^4A_g \rightarrow ^4T_g$ (ν_1) and $^4A_g \rightarrow ^4T_1g$ (ν_2) transition, respectively. ν_3 , B₂, β and 10 Dq were calculated by using Tanabe-Sugano diagram for d³ configuration (Table 4). The magnetic moment values was recorded (3.21, 3.36 and 3.27) BM respectively which refer to three electron of paramagnetic for chromium (III) agree with octahedral geometries around Cr(III) ion (Pahontu *et al*, 2018). The conductance measurement indicated the non-ionic behavior for all these prepared complexes.

PdL₁ and PdL₂

The electronic spectra of brown complexes show bands at (24154 and 23809) cm⁻¹ for PdL₁ and PdL₂ which attributed to $^1A_1g \rightarrow ^1B_1g$ transition (ν_1) and at (26246 and 32258) cm⁻¹ is due to $^1A_1g \rightarrow ^1E_g(i_2)$ transitions respectively for square planer geometry (Alias and Bakir, 2018). Another bands appeared at (31746 and 35460) cm⁻¹ can be assigned to charge transfer L \rightarrow PdCT transition for L₁ and L₂ respectively (Alias and Bakir, 2018). The measured magnetic moment is zero B.M. showed that the complexes to be low spin, and the conductivity measurements indicted that the both complexes are nonionic (Alias and Bakir, 2018).

PtL₁ and PtL₂

Two principle spin-allowed absorption bands at (37037, 26525) and (35087, 26315)cm⁻¹ for PtL₁ and PtL₂ respectively are to be expected corresponding to the transition from the 1A_1g ground state to 1T_1g and 1T_2g excited states and in addition, the band assigned to the spin forbidden singlet–triplet transition may be observed at lower energies then spin allowed transition which assign to the $^1A_1g \rightarrow ^3T_1g$, 3T_2g (Mahasin *et al*, 2016). The colors complexes shows bands in UV region may berefer to change transfer from donor atoms of the ligand to the platinum charge transfer L \rightarrow PtCT transition. The magneticmoment for both complexes is diamagnetic and the conductance measurements indicate the non-ionic behavior of these complexes (Table 4). From these results and others studies on geometries can be suggested for these complexes.

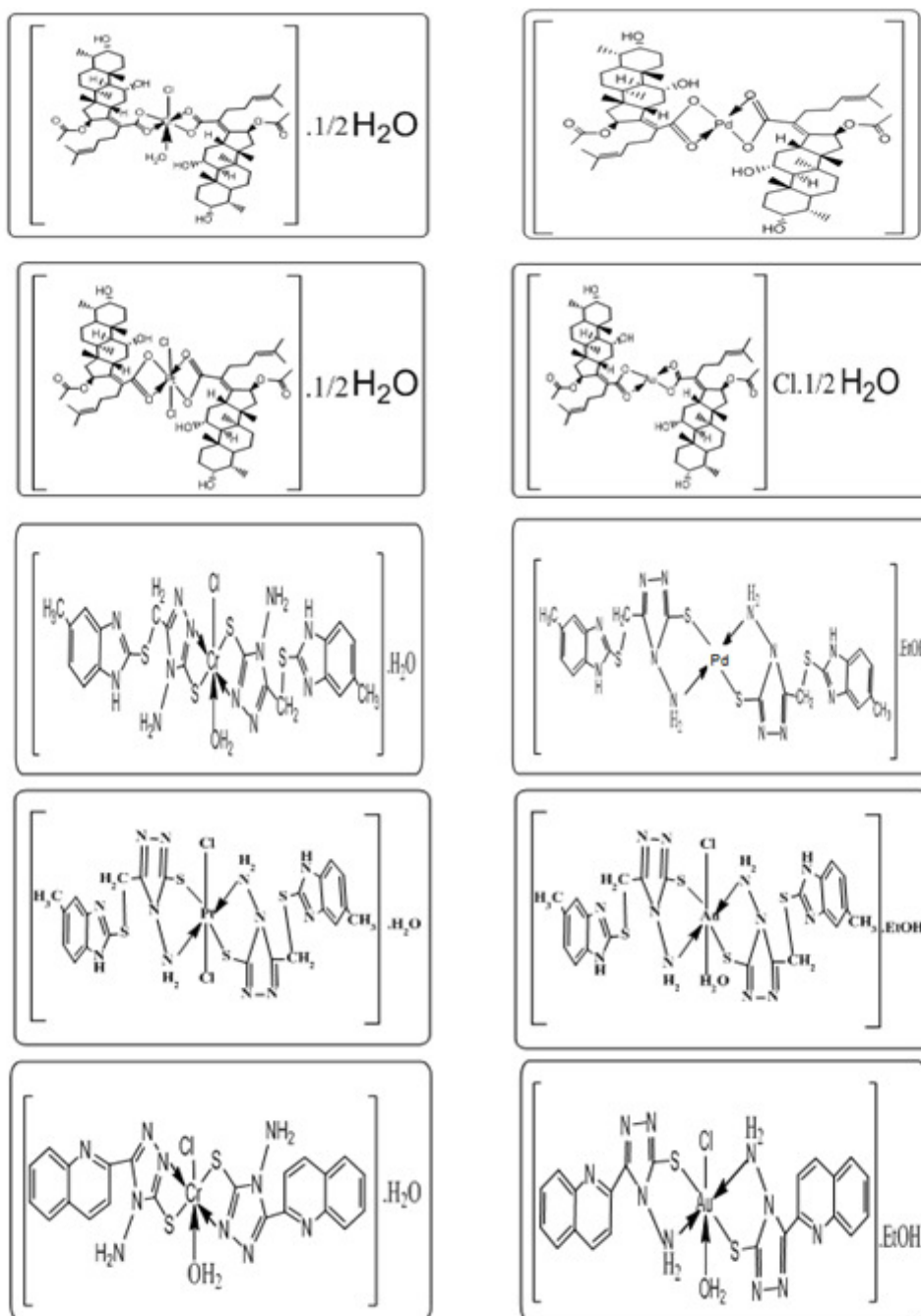
AuL₁

In this work, diamagnetic of the gold complex exhibited two bands one at 27027 cm⁻¹ which corresponding to the $^1A_1g \rightarrow ^1B_1g$ transition (ν_1), and the other band appeared at 34482cm⁻¹ which assigned to $^1A_1g \rightarrow ^1E_g$ transition (ν_2) in square planner geometry (Alias and Abdul Hassan, 2015), the conductivity measurement for this complex showed to be ionic behavior

Table 9 : Statistical data and IC_{50} values of L_3 and its metal complexes as well as control positive on MDA-231 cells lines in time of exposure 48 hrs.

Conc.	Inhibition rate% (means \pm standard deviation \pm SD)				
	Cis -platin	Ligand 3	CrL3	AuL3	LSD value
400	73.78 \pm 1.08aB	64.16 \pm 1.08aC	77.66 \pm 2.09aB	82.09 \pm 1.00aA	3.912 *
200	61.91 \pm 1.11bB	60.39 \pm 0.77bB	71.39 \pm 0.83bA	52.25 \pm 2.83bC	4,.362 *
100	51.00 \pm 1.12cB	56.97 \pm 1.55cA	49.99 \pm 0.86cB	40.25 \pm 1.22cC	4.689 *
50	46.09 \pm 0.69dA	48.99 \pm 0.99dA	31.99 \pm 0.72dB	33.47 \pm 1.28dB	4.305 *
25	32.89 \pm 1.68eB	38.94 \pm 0.98eA	22.98 \pm 0.85cC	29.87 \pm 0.98eB	4.684 *
LSD value	2.149 *	2.032 *	2.164 *	2.951 *	—
IC_{50}	41.77	47.12	34.36	31.82	—

Means having with the different letters in same column differed significantly, * ($P < 0.05$).

**Fig. 1 :** The suggested structure of New prepared Complexes.

(Table 4).

AuL₂ and AuL₃

Gold (III) complexes is in high crystal field effect due to the large size of gold (III) ion, being in the third transition series beside to higher oxidation state of these metal ion (Alias and Abdul Hassan, 2015). The electronic spectra of these color complexes exhibit two bands (25974, 28985) cm⁻¹ for L₂ and (25641, 30303) cm⁻¹ for L₃ which assignment to ³A₁g→³T₂g, ³A₁g→³T₁g transition and other bands at highest wave number which corresponding to the charge transfer (Alias and Abdul Hassan, 2015). The ν₃ and the ligand field parameter were calculated using Tanabe-Sugano diagram d⁸ for oh system. The values in Table 4 which shows approximately agree with oh environment which reported (Alias and Abdul Hassan, 2015). The magnetic moment of these complexes are (2.66 & 2.54) B.M. and the conductance measurements indicate the non-ionic behavior for these complexes. From these results and other studies oh geometries can be suggested for gold(III) complexes.

¹HNMR and ¹³CNMR spectra:

Mode of the ligands and their complexes are also provided by the ¹HNMR and ¹³CNMR spectra, which were recorded in DMSO d₆ shown in Tables 5 & 6.

The proposed structure model for these newly prepared complexes which is characterized by physical and spectroscopic analysis can be shown Fig. 1.

Cytotoxic assay

From last few decades the breast cancer is one of the major issues in health care in terms of morbidity, mortality and therapy costs (Benson *et al*, 2009). In addition, although many more drugs have been introduced into the market but the response to therapy is still poor. Therefore, there is an urgent need for more efficient anticancer drugs to be developed. The foremost target of most research groups is to find a convenient anticancer drug that can be used efficiently for the treatment of human tumors (Abu-Surrah *et al*, 2010). MTT assay was applied to assess cytotoxicity and viability of the MDA-231 cell lines after 48 hrs of the treatment with the compounds at different concentrations (400, 200, 100, 50 and 25 µg/ml) (Tables 7-9 and Figs. 2-4. MTT assay results showed a high inhibition rates for all ligands and their metal complexes using different doses and compared with the cis-platin as control positive, the statistical results showed that the three ligands were significant effect when compared to control positive (cis-platin). Linear regression analysis with 95% confidence limit was used to define dose-response curves and the inhibition rates began to

reduce gradually from high to low concentrations and in significant difference (P<0.05) at all concentrations and comparable to control positive and ligand when compare with cis-platin recorded. The mechanism of action of the prepared complexes remained unclear. From the results presented in this work many factors may be responsible about the activity of these complexes in pharmacological field like size of metal, charge distribution, geometry shape, bond character, polarity, oxidation state of metal and design of substitution of organic compounds.

In the L₁ and L₂ complexes, it can be explained that palladium complexes has higher toxicity than other prepared complexes may be due to their structural square planar geometry, owing to its chemical properties and coordination modes similar to platinum(II), palladium(II) has attracted great interest in terms of anticancer potential (Garoufis *et al*, 2009). Both metals in the +2 oxidation state generate square-planar complexes. On the other hand, palladium(II) derivatives are thermodynamically and kinetically less stable than the platinum(II) counterparts, and undergo aquation and ligand exchange much faster, thus limiting their medicinal applications (Serebryanskaya *et al*, 2013). Therefore, an appropriate design of the ligands, including the development of glycoconjugates, would allow the tuning of hydrolysis rates. Importantly, a good relationship was observed between the cytotoxic activity of the Pd complexes and their lipophilicity or solubility (Garoufis *et al*, 2009; Serebryanskaya *et al*, 2013). In fact, Pd complexes, as non-platinum complexes, have recently been reviewed to have a significant anti-tumour activity to cancer cells as well as lower side effects compared to cisplatin such as nephrotoxicity, drug resistance, renal and cervical problems (Kollur *et al*, 2013; Geo *et al*, 2009). As an important feature of metal-containing anti-cancer agents, Pd complexes are expected to have less kidney toxicity than cisplatin (Kollur *et al*, 2013). Among non-platinum anticancer agents, gold derivatives are currently gaining ground as a new class of potential chemotherapeutics owing to their capability to inhibit tumor cell growth through non-cisplatin-like mechanisms of action (Nardon *et al*, 2014). Gold complexes with reported antiproliferative properties include different ligands bound to the metal center in either +1 or +3 oxidation states. Gold(III) shares some important chemical features with platinum(II), such as the typical square-planar coordination geometry and the same d⁸ electronic configuration, thus making it very attractive for the development of alternative antineoplastic drugs (Nagy *et al*, 2012) and this illustrated to the highly inhibition rates of gold (III) complexes which synthesized in this paper. Chromium(III) chelates have been found to

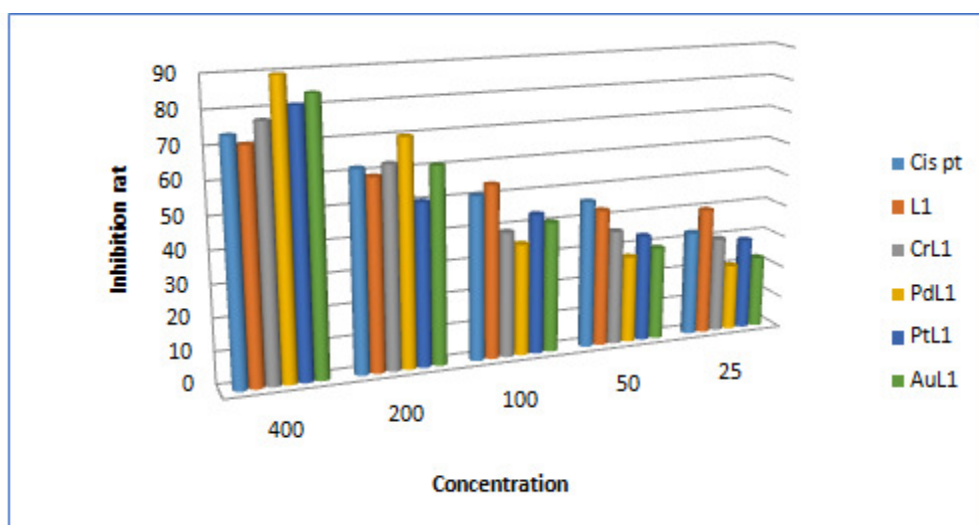


Fig. 2 : The percentage of inhibition rate on MDA-231 cell line after exposure to CrL₁, PdL₁, PtL₁ and AuL₁ complexes for 48 hrs compared to control positive (Cis-Pt) and the ligand.

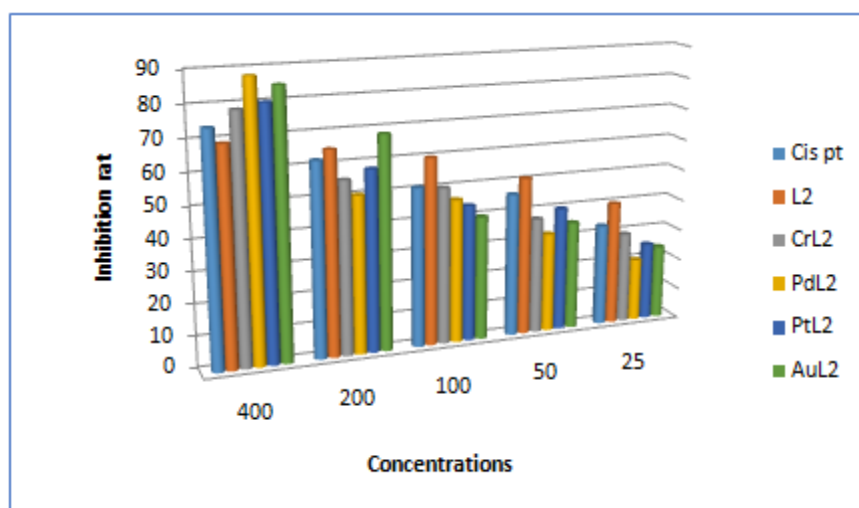


Fig. 3 : The percentage of inhibition rate on MDA-231 cell line after exposure to CrL₂, PdL₂, PtL₂ and AuL₂ complexes for 48 hrs compared to control positive (Cis-Pt) and the ligand.

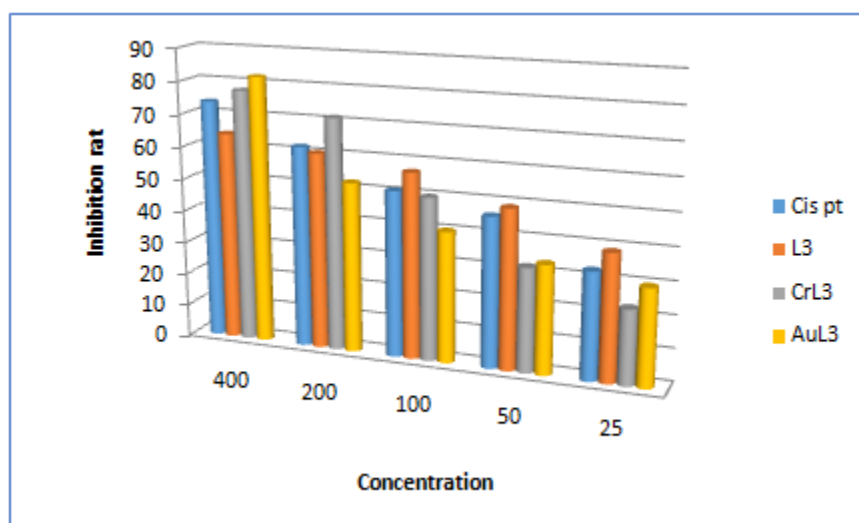


Fig. 4 : The percentage of inhibition rate on MDA-231 cell line after exposure to CrL₃ and AuL₃ complexes for 48 hrs compared to control positive (Cis-Pt) and the ligand.

interact with biological systems and to exhibit anti-neoplastic activity and antibacterial, antifungal and anticancer activity. Some chromium (III) N,S,O/N,N-donor chelators are good anticancer agents due to strong binding ability with DNA base pair (Ghssein and Matar, 2018; Abdel-Rahman *et al*, 2017) and this illustrated the high inhibition rates of this complexes in this study.

CONCLUSION

The synthesized compounds are promising as new anticancer candidates in future especially in high concentration.

REFERENCES

- Abdel-Rahman L H, Abu-Dief A M, Aboelez M O and Abdel-Mawgoud AA (2017) DNA interaction, antimicrobial, anticancer activities and molecular docking study of some new VO (II), Cr (III), Mn (II) and Ni (II) mononuclear chelates encompassing quaridentate imine ligand. *J. Photochem. Photobiol. Biol.* **170**, 271–285.
- Abdnoor Z M and Alabdali A J (2019) Synthesis, characterization, and anticancer activity of some azole heterocyclic complexes with gold (III), palladium (II), nickel (II) and copper (II) metal ions. *J. Chinese Chem. Soc.* **66**, 1–10.
- Abdullah B H, Abdullah M A, Al-Jibori S A and Talal A K (2007) Platinum (II) Linkage Isomeric Complexes Containing Mixed Ligands 4, 5-diphenyl-1, 2, 4-triazole-3-thione and Diphosphines $\text{Ph}_2\text{P}(\text{CH}_2)_n\text{PPh}_2$ ($n = 1, 2$ or 3). *Asian J. Chem.* **19**(2), 1334.
- Abu-Surrah A S, Abu Safieh K A, Ahmad I M, Abdalla M Y and Ayoub M T (2010) New palladium(II) complexes bearing pyrazole-based Schiff base ligands: Synthesis, characterization and cytotoxicity. *Eur. J. Med. Chem.* **45**, 471–475.
- Al-Dulimia A A A, Al-Hasani R A and Yousif E A (2016) Synthesis, Characterization, Theoretical studies and Photostabilization of Mefenamic acid Derivative with some divalent metal ions. *European Chemical Bulletin* **5**(10), 456–464.
- Alias M and Bakir S R (2018) Synthesis, Spectroscopic Characterization and *in Vitro* Cytotoxicity Assay of Morpholine Mannich Base Derivatives of Benzimidazole with Some Heavy Metals. *Al-Nahrain J. Sci.* **21**(3).
- Alias M F (2007) Synthesis and characterization of some new metal complexes with Bis [4-phenyl-2-dibutyl aminomethyl-1,2,4-triazole-3-thion-5yl]methane and theoretical study. *Al-Nahrain J. Sci.* **10**(2), 13–24.
- Alias M F and Abdul Hassan M M (2015) Synthesis and Characterization of Some Metal Complexes with their Sulfamethoxazole and 4, 4'-dimethyl-2, 2'-bipyridyl and study Cytotoxic Effect on Hep-2 Cell Line. *Baghdad Sci. J.* **12**(4), 740–752.
- Alias M F, Hashim A J and Kareem T A (2008) Synthesis and Characterization of Some Inorganic Compounds and Study their Effect in activity of Laccase Produced by Fungal isolate *Pleurotus ostreatus*. *Ibn AL-haitham J. Pure Appl. Sci.* **21** (2).
- Alias M, Ismael S and Mousa S A (2015) Synthesis, Characterization and Theoretical Study of Some Mixed-ligand Complexes of 2-Quinoline Carboxylic Acid and 4, 4D -dimethyl, 2, 2D -Bipyridyl with Some Transition Metal Ions. *Al-Nahrain J. Sci.* **18**(1), 28–38.
- Al-Maydama H M, Al-Ansi T E Y and Ali A H (2008) *Ecl. Quim. Sao. Paulo.* **33**(3), 29–42.
- Baile M B, Kolhe N S, Deotarse P P, Jain A S and Kulkarni A A (2015) Metal ion complex-potential anticancer drug-a review. *Int. J. Pharma Res. Rev.* **4**(8), 59–66.
- Benson J R, Jatoti I, Keisch M, Esteva F J and Makris A (2009) Early breast cancer. *Lancet* **373**, 1463–1479.
- Bhola Y, Naliapara A, Modi J and Naliapara Y (2019) Synthesis and biological activity of pyrazole and 1, 2, 3-triazole containing heterocyclic compounds. *World Scientific News* **117**, 29–43.
- Chen D, Lin X X, Zhao Q, Xiao J, Peng S F, Xiao M F and Zhang W (2017) Screening of drug metabolizing enzymes for fusidic acid and its interactions with isoform-selective substrates *in vitro*. *Xenobiotica* **47**(9), 778–784.
- Curbete M M and Salgado H R N (2016) A critical review of the properties of fusidic acid and analytical methods for its determination. *Critical Rev. Anal. Chem.* **46**(4), 352–360.
- Deacon G and Phillips R (1980) Coordination Chemistry. *Review* **33**, 227–250.
- Fathima K S, Sathiyendran M and Anitha K (2019) Structure elucidation, biological evaluation and molecular docking studies of 3-aminoquinolinium 2-carboxy benzoate-A proton transferred molecular complex. *J. Mol. Structure* **1176**, 238–248.
- Fernandes P (2016) Fusidic acid: a bacterial elongation factor inhibitor for the oral treatment of acute and chronic staphylococcal infections. *Cold Spring Harbor Perspectives in Medicine* **6** (1), a 025437.
- Gao E, Liu C, Zhu M, Lin H and Wu Q (2009) Current development of Pd (II) complexes as potential antitumor agent. *Anticanc Agents Med. Chem.* **9**, 356–368.
- Garoufis A, Hadjikakou S K and Hadjiliadis N (2009) Palladium coordination compounds as anti-viral, anti-fungal, anti-microbial and anti-tumor agents. *Coord. Chem. Rev.* **253**, 1384–1397.
- Ghssein G and Matar S (2018) Chelating mechanisms of transition metals by bacterial metallophores “Pseudopaline and Staphylopine”: a quantum chemical assessment. *Computation* **6**, 56.
- Gobouri A A, Alshanbari N A, Mohamed M A and Abdel-Hafez S H (2019) One pot synthesis of ethyl carboxylate and acetyl selenolo [2, 3-b] quinoline derivatives and their tetra/pentacyclic systems. Phosphorus, Sulfur and Silicon and the Related Elements, pp.1–7.
- Joshi R, Kumari A, Singh K, Mishra H and Pokharia S (2019) New diorganotin (IV) complexes of Schiff base derived from 4 amino 3 hydrazino 5 mercapto 4H 1, 2, 4 triazole: Synthesis, structural characterization, density functional theory studies, atoms in molecules analysis and antifungal activity. *Appl. Organometallic Chem.* **33**(5), e 4894.
- Kollur S P, Linganna S K, Shivamallu C, Naveen Kumar R M and Revanasiddappa H D (2013) Palladium(II) complexes as biologically potent metallo-drugs: Synthesis, spectral characterization, DNA interaction studies and antibacterial activity. *Spectrochim Acta Part A* **107**, 108–116.
- Lotfy H M, Salem H, Abdelkawy M and Samir A (2015) Spectrophotometric methods for simultaneous determination of betamethasone valerate and fusidic acid in their binary mixture. *Spectrochimica Acta Part A: Molecular and Biomolecular Spectroscopy* **140**, 294–304.

- Magee C N, Medani S A, Leavey S F, Conlon P J and Clarkson M R (2010) Severe rhabdomyolysis as a consequence of the interaction of fusidic acid and atorvastatin. *Am. J. Kidney Dis.* **56**(5), e11-e15.
- Mahasin F A, Basha'ar A S and Farah S J (2016) Coordination of Some Heavy Transition Metals Complexes with 2- amino Acetic Acid-6-Methoxy Benzothiazole Using Microwave and Thermal Methods. *Int. J. Pharm.* **6**(1), 6-13.
- Mishra K K, Ahmad A and Srivastava K P (2019) Synthesis, characterization and anti-microbial activity of transition metal (II) complexes with bidentate (N & S donor) thioamide ligand. *Int. J. Scientific Res. Review* **7**, 1813-1820.
- Nagy E M, Ronconi L, Nardon C and Fregona D (2012) Noble metaldithiocarbamates: precious allies in the fight against cancer, *Mini-Rev. Med. Chem.* **12**, 1216-1229.
- Nakamoto N (2009) *Infrared and Raman Spectra of Inorganic and Coordination Compounds*. John Wiley & Sons, Inc., 6th Ed., New York.
- Nardon C, Boscutti G and Fregona D (2014) Beyond platinum: gold complexes as anticancer agents. *Anticancer Res.* **34**, 487-492.
- Nevade S A, Lokapure S G and Kalyane N V (2013) Synthesis and Pharmacological Evaluation of Some Novel 2-Mercapto Benzimidazole Derivatives. *J. Korean Chem. Society* **57**(6), 755-760.
- Pahontu E, Usataia I, Graur V, Chumakov Y, Petrenko P, Gudumac V and Gulea A (2018) Synthesis, characterization, crystal structure of novel Cu (II), Co (III), Fe (III) and Cr (III) complexes with 2 hydroxybenzaldehyde 4 allyl S methylisothiosemicarbazone: Antimicrobial, antioxidant and in vitro antiproliferative activity. *Appl. Organometallic Chem.* **32**(12), e 4544.
- Park M R, Kim D S, Kim J and Ahn K (2013) Anaphylaxis to topically applied sodium fusidate. *Allergy, Asthma & Immunology Research* **5**(2), 110-112.
- Scozzafava A, Cavazza C, Supuran C T, Saramet I, Briganti F and Banciu M D (1998) Complexes with Biologically Active Ligands. Part 111. Synthesis and Carbonic Anhydrase Inhibitory Activity of Metal Complexes of 4, 5-Disubstituted-3-Mercapto-1, 2, 4-Triazole Derivatives. *Metal-based drugs* **5**(1), 11-18.
- Serebryanskaya T V, Yung T, Bogdanov A A, Shchebet A, Johnsen S A, Lyakhov A S, Ivashkevich L S, Ibrahimava Z A, Garbuzenco T S, Kolesnikova T S, Melnova N I, Gaponik P N and Ivashkevich O A (2013) Synthesis, characterization, and biological evaluation of new tetrazole-based platinum(II) and palladium(II) chlorido complexes - Potent cisplatin analogues and their trans isomers, *J. Inorg. Biochem.* **120**, 44-53.
- Skooze D A, West D M and James H F (2014) *Fundamentals of analytical chemistry*. 9th Ed., Brooks \Cole.
- Statistical Analysis System (SAS) (2012) User's Guide. Statistical. Version 9.1th ed. SAS. Inst. Inc. Cary. N.C. USA.
- Steinkraus G E and McCarthy L R (1979) *In vitro* activity of sodium fusidate against anaerobic bacteria. *Antimicrobial Agents and Chemotherapy* **16**(2), 120-122.
- Symal A and Bari Niazi M A (1984) Synthesis of new Schiff bases derived from 4-amino-5-mercapto-3-methyl-1,2,4-triazole & salicylaldehyde or substituted salicylaldehyde & their copper(II) complexes. *Indian J. Chem.* **23A**, 163-165.
- Verbanac D, Malik R, Chand M, Kushwaha K, Vashist M, Matijašić M and Jain S C (2016) Synthesis and evaluation of antibacterial and antioxidant activity of novel 2-phenyl-quinoline analogs derivatized at position 4 with aromatically substituted 4 H-1, 2, 4-triazoles. *J. Enzyme Inhibition and Medicinal Chem.* **31**(sup2), 104-110.
- Whitby M (1999) Fusidic acid in the treatment of methicillin-resistant *Staphylococcus aureus*. *Int. J. Antimicrobial Agents* **12**, S67-S71.
- Xiao Q Q, Liu D, Wei Y L and Cui G H (2019) Two new ternary Mn (II) coordination polymers by regulation of aromatic carboxylate ligands: Synthesis, structures, photocatalytic and selective ion-sensing properties. *J. Solid State Chem.* **273**, 67-74.
- Zhang P Z, Zhou S F, Li T R and Jiang L (2012) Efficient synthesis and *in vitro* antifungal activity of 1H-benzimidazol-1-yl acetates/propionates containing 1H-1, 2, 4-triazole moiety. *Chinese Chemical Letters* **23**(12), 1381-1384.